Electrospinning and Optical Properties of Polyacrylonitrile/Titanium Dioxide Nanocomposite Fibers

Farah M. Radee [1], Widad S. Hanoosh[2] and Ali Q. Abdullah[1,*]

1. Department of Physics, College of Science, University of Basrah, Basra, IRAQ.
2. Department of Chemistry, College of Science, University of Basrah, Basra, IRAQ.

*Corresponding author: E-mail: ali.abdullah@uobasrah.edu.iq

Doi: 10.29072/basjs.20230209

ARTICLE INFO

Keywords

Electrospinning, Polyacrylonitrile, Nanofibers, Titanium dioxide, Energy gap, volume and surface energy loss functions.

ABSTRACT

In situ polymerization was used in this work to prepare polyacrylonitrile (PAN) and titanium dioxide (TiO2) nanocomposite at various ratios (5, 10, 15, and 20 weight percent of TiO2). PAN/TiO2 nanofibers were created using the electrospinning process from a homogenized solution. X-ray diffraction data demonstrated that a structural change to an amorphous state had taken place. Using scanning electron microscopy (SEM), the morphology of the high-aligned fibers with PAN diameters of roughly 33 nm and 51 nm of PAN/(10wt%)TiO2 was examined. A spectrophotometer was used to examine the optical characteristics of the nanofiber films at wavelengths between 200 and 900 nm. The energy gap (Eg) of the nanofiber films was computed, and it decreased as the weight ratio of the TiO2 nanoparticle increased. With 5, 10, and 15% weight percentage of TiO2, respectively, the energy gap (Eg) of PAN nanofibers changes from 3.92 eV to 3.72, 3.39, 3.19 eV. Several other parameters have also been calculated, including the excitation coefficient (k), refractive index (n), Urbach tail (Et), dielectric constant (ε_1), dielectric loss (ε_2), and volume and surface energy loss functions (VELF) and (SELF).

Received 19 Feb 2023; Received in revised form 27 Mar 2023; Accepted 3 July 2023, Published 31 Aug 2023

1. Introduction

Electrospinning is an easy and cheap process for producing composite nanofibers. These membranes have a high surface area for volume[1]. The electrospinning device consists of four basic parts: a syringe for placing the polymeric solution into it, a metal needle, a power supply and a conductive collector (fixed or movable). The process of producing nanofibers starts by electrospinning when electric charges are transmitted to a polymeric material solution through the conductive injector head. Which generates instability inside the polymer solution as a result of the diffusion of charges on the polymer droplet. At the same time, the mutual repulsion of charges produces a force opposing the surface tension, which causes the polymer solution to flow in the direction of the electric field. When the applied electric field is able to overcome surface tension of the polymeric solution, the drop changes from spherical to conical, forming a Taylor cone, in this step, nanofibers are produced from a polymer droplet (Taylor cone). The fibers are assembled on the mineral collector placed at an appropriate distance. The electric field between the metal syringe and the collector elongates the jets towards the collector. As a result of the above, fibers with nano-diameters are produced [2]. In electrospinning, it is possible to control the properties of nanofibers to obtain the required properties for use in the desired application, and this is done by controlling the parameters of the polymeric solution such as:, applied conductivity, viscosity of polymer, or by adjusting the electrospinning process parameters, such as the flow rate voltage and the distance between injector head and accumulator[3]. In most cases, the goal of the electrospinning process is to obtain smooth, uniform, bead-free fibers with nano-diameters[4]. The most important properties of nanofibers are good mechanical properties, flexibility and high surface area to volume ratio [5]. Nanofibers were produced using different types of materials, and polymers are among the most used materials in the electrospinning process, and many nano-dimensional materials are introduced into the polymeric solution such as (nanoparticles, nanorods, nanowires, nanotubes, and nanosheets). Electrospun it directly into the nanofibers[6]. One of these polymers is PAN, Polyacrylonitrile fiber ranks third among all other types of synthetic fiber production. This is due to its unique properties such as mechanical strength and chemical resistance[7]. It is used in the manufacture of army special clothing, medical and antibacterial clothing, ultra-water-resistant membranes, electrical appliances, optoelectronic devices, and energy storage systems[7]. Optical measurements show a good method for examining semiconductor properties, This involves calculating the absorption coefficient for a variety of

energies, Which gives the researcher an explanation of the energy gap of matter. The energy difference between orbitals shows the number of atoms and the nature of the bonding system. To understand the electrical properties of semiconductors, the energy gap must be calculated, So it is of great practical importance. In order to implement a specific design with high accuracy using a variety of polymeric materials, the refractive indices are controlled by design [8]. In the current work polyacrylonitrile (PAN) mixed with Titanium dioxide (TiO_2) nanoparticles with different weight ratios (5%,10%,15%). The absorbance was measured with UV-Vis spectroscopy. The measurements were analyzed and discussed.

2. Experimental procedure

Tetraethylorthosilicat (TEOS, 98 %) from Sigma-Aldrich, Germany. Trimethylchlorosilane (TMCS, > (98%) TCI Japan. Hexane (> 98%), from the Chem-Lab (Belgium). Schariau Ethanol (Spain) > (99%) Hydrochloric acid (35-38%), from Thoma Baker (India). Ammonia Solution from CDH (India). Prepare the silica (sol, gel, modified gel, and aerogel doped with metal ions in 10^{-2} gm/cm ^{3}, and dissolved copper chloride (CuCl) by add 0.085g in 50ml ethanol. In the first step Condensed silica (CS) as a precursor, TEOS was mixed with ethanol to create condensed silica with a molar ratio of TEOS 20ml was mixed with 40ml ethanol and on a magnetic stirrer for 10 minutes and then 2ml (0.1M HCl) as an acidic catalyst. Preparation stage sol 5ml of copper chloride was mixed with 10ml) of condensed and then the each Add the base catalysis (0.5M NH_4OH) and stir in a magnetic field for 15 minutes to turn the sol into a gel. The gel is aged for two hours after being prepared for 15 minutes, then rinsed in ethanol three times every 24hr's. Surface modification was achieved by combining TMCS 7.5ml with hexane 30ml . and applied to the gel put in the oven at 60℃ for 24hr's. then it is placed in hexane soaked for 24hr's. at room temperature, exchanged with pure hexane at 60℃ for 4hr. then exchanged with pure hexane at room temperature and washed in pure hexane and covered the holder in selofin with tiny holes and let them to dry at room temperature. put the gel in the oven at temperatures up about 180℃ gradually every 20 ℃ until they dry.

2. Materials and methods:

2.1 Materials

Acrylonitrile monomer (AC) (99.34%, Fluka), N-Dimethylformamide (DMF) (99.9%, BDH), Ammonium Persulfate (APS), Serfcant (S), deionized water, Titanium dioxide (TiO_2) nanoparticle

was supplied from Sigma Aldrich, with the following specification: [Color pure white, Particle size (23-25) nm], all material used without any purification.

2. 2 Syntheses PAN / TiO_2 in situ

Required amounts of AC monomer in deionized water was prepared, then determine quantities of TiO_2 nanoparticles (5,10 and 15) wt% were added to the solution above and sonicated for 1 hour before adding initiator and surfactant. 0.5g APS and 0.3 g surfactant were added to the solution and reflux for 1hr.

2.3 Electrospinning of PAN polymeric solution and PAN/TiO_2 composites:

The nanofibers were prepared by the electrospinning process of PAN and PAN/TiO_2 by using 3% of PAN by dissolved in (DMF), and by continuous stirring of the solution for a full day at room temperature to obtain a homogeneous solution. The polymeric solution is placed in a 3ml (24 g) plastic syringe, applying a high voltage (10 KV), the flow rate of the polymeric solution is 1 mL/hr. and the space between the metal syringe and the collector is 10 cm. The same previous process was used, but by adding TiO_2 to PAN with different weight percentages (5,10 and 15%), respectively, and treating the solution with ultrasonic for two hours to ensure the homogeneity of the solution. All tests were performed at room temperature. Figure 1 shows a chemical structure of PAN and a diagram of the electrospinning device[9].

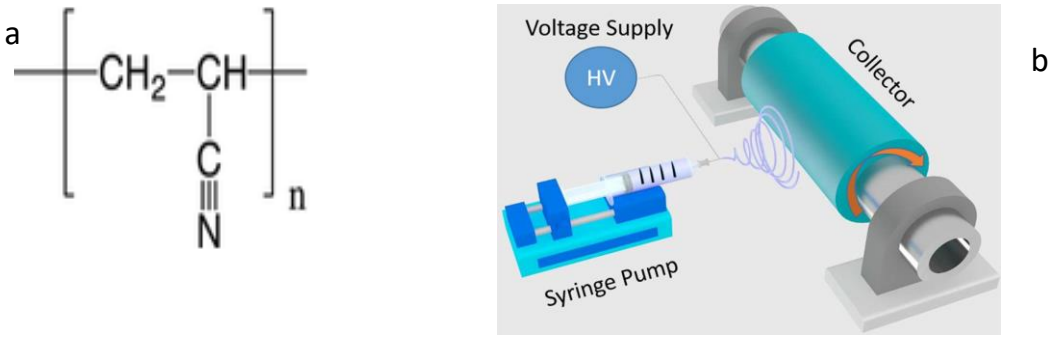

Figure 1: (a) The chemical structure of PAN and (b) The Scheme of the electrospinning device[8].

3. Characterization of PAN and PAN/TiO_2 Nanocomposite

X-ray diffraction measurements were carried out to investigate the change of crystalline state of PAN before and after the addition of TiO_2. Figure 2 shows the XRD of the nanofibers prepared for both PAN and PAN/TiO_2. Three peaks can be observed indicating the semi-crystalline structure of PAN, the first peak at 17.1, this is what Chris Ademola and his group indicated[10], for PAN/TiO_2 fibers, we notice amorphous structure well dominated .

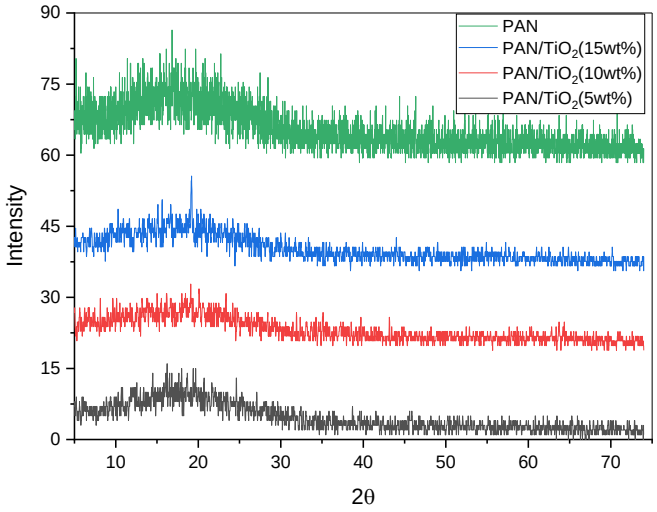

Figure 2: XRD of PAN and PAN/TiO_2 at different weight ratios

3.2 Scanning Electron Microscopy (SEM)

The thin film PAN nanofiber morphology was studied. Figure 3 shows a scanning electron microscope (FEI NOVANanosem 4501, Japan). SEM images are presented the average fiber diameter 33 nm for PAN as shown in Figure 3 (a), while the average diameters in PAN/TiO_2 (10wt%) nanocomposite were about 51 nm as shown in Figure 3 b. The aligned nanofibers were clearly because we using rotation speed about 1247rpm for drum collector [11], also the concentration of the solution is the most important factor influencing the diameter of nanofibers [12]

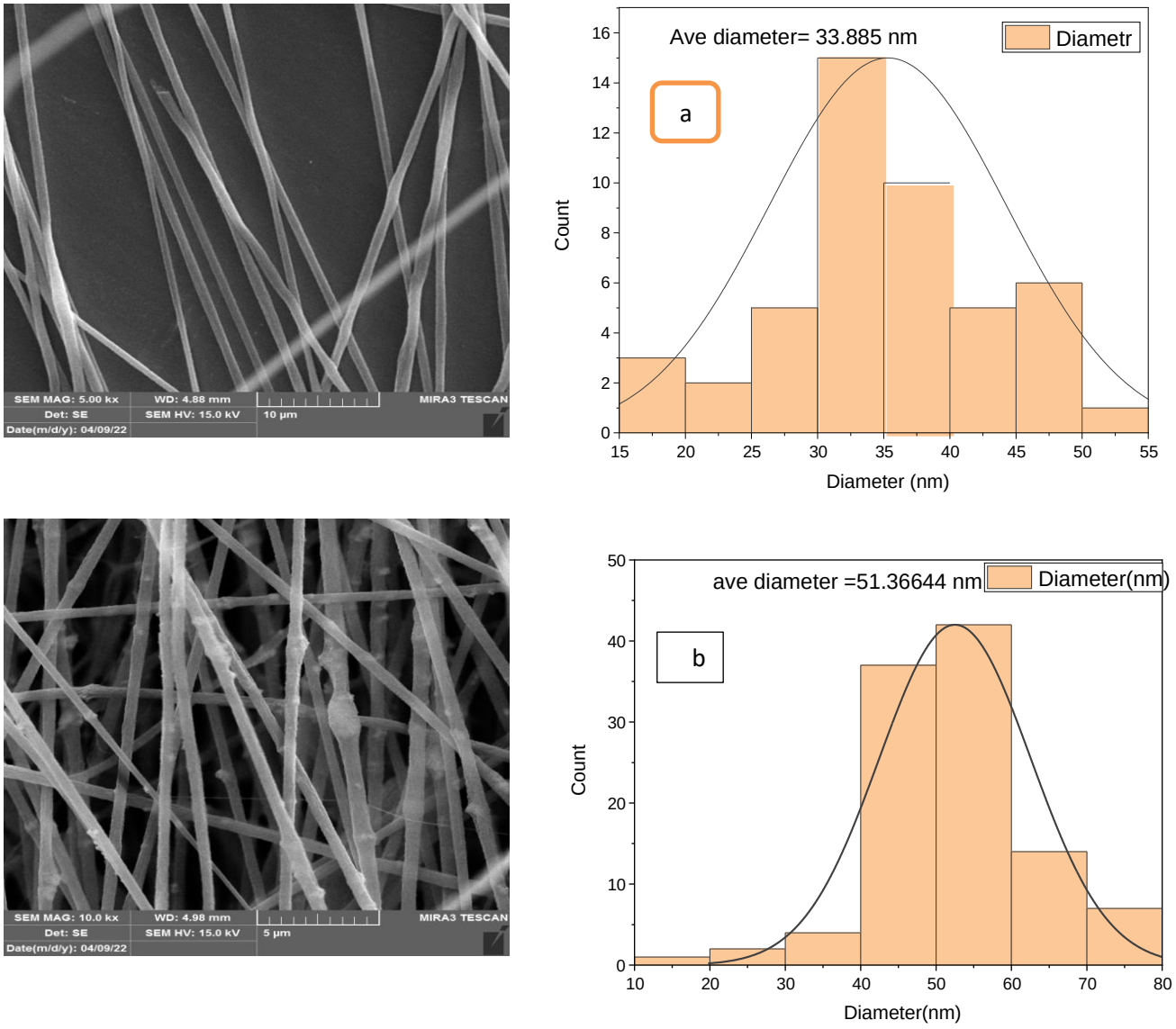

Figure 3: SEM for(a) PAN and (b) PAN /TiO_2 (10wt%) nanocomposite

3.3 Optical properties analysis

Optical properties analysis of the obtained nanofibers, it was performed on the basis of the recorded absorbance spectra of electromagnetic radiation for wavelengths range (200 - 900 nm). The occurrence of absorption in the ultraviolet region each of the polyacrylonitrile (PAN) nanofibers and the polymeric composite nanofibers (PAN/TiO_2). Absorption spectra (A) of PAN and PAN/ TiO_2 nanocomposite fiber at different ratios (5, 10,15) wt % TiO_2 was illustrated in Figure 4

respectively. There is a sharp edge of the absorbance spectrum at the ultraviolet region (250 - 300) nm associated with the transition n - π* [12]. In addition, the absorption decreases with increasing wavelength due to the weak absorption in the region above 400 nm[13].

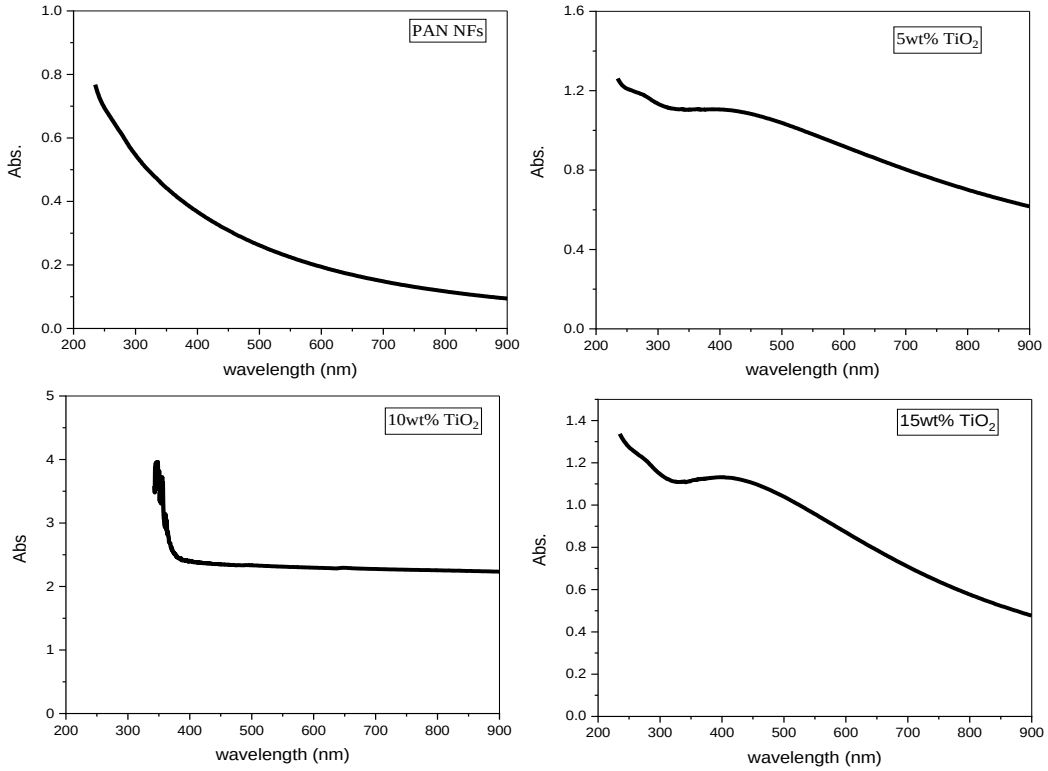

Figure 4: Absorbance spectrum at different wavelength of PAN and PAN/TiO_2 nanofibers

The relationship between normal-incidence reflectivity (R) and wavelength as shown in Figure 5 of PAN and PAN/TiO_2 nanofibers .From figures we noticed decreasing in reflectivity with increases in wavelength (λ) , while increasing in reflectivity (R) at increase the weight ratios of TiO_2 .

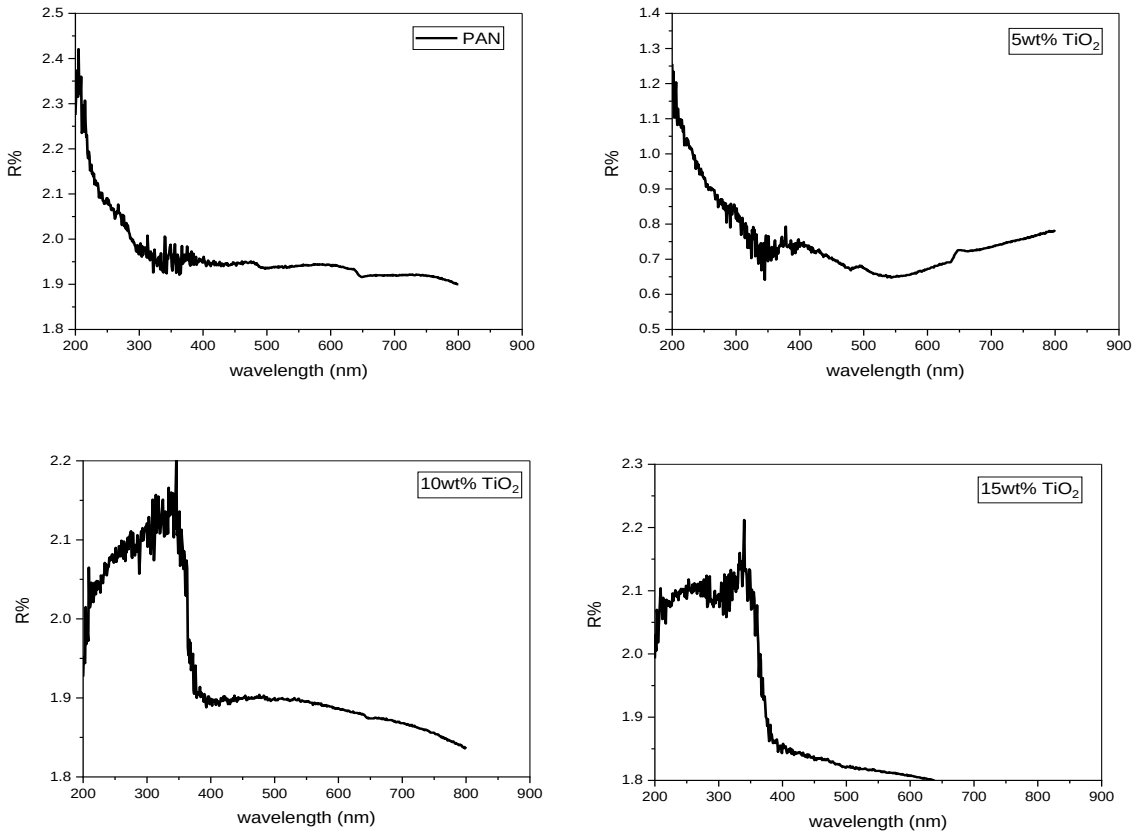

Figure 5 : Reflectivity (R) as a function wavelength (λ) of PAN and PAN/TiO_2 nanofibers

To calculate the absorption coefficient α we use the equation[14]:

$$\alpha = 2.303 \frac{A}{d} \text{ ……..1}$$

where d: nanofiber thin film thickness.

The absorption coefficient (α) as a function of photon energy(hν) is shown in the Figure 6 of the prepared nanofibers for PAN and PAN/ TiO_2 nanocomposite fibers with different weight ratios (5,10 and 15) wt% TiO_2.

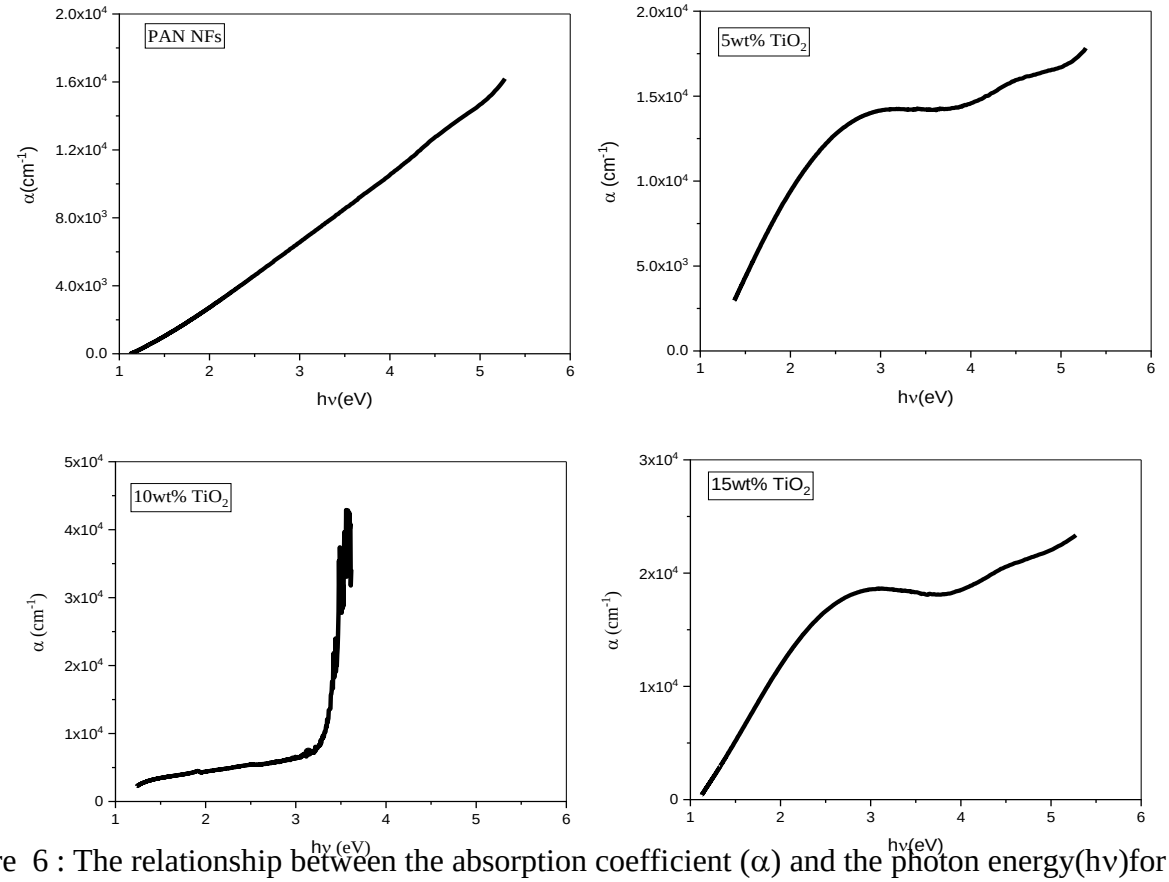

Figure 6 : The relationship between the absorption coefficient (α) and the photon energy(hν)for PAN and (PAN/TiO_2) nanofibers

The excitation coefficient (k) is the amount of energy absorbed in the matter. The electrons of matter formed from the energy of the incident photons . Electromagnetism within matter. The excitation coefficient (k) is given by the relationship[14]:

$$K = \frac{\alpha\lambda}{4\pi} \qquad \ldots\ldots\ldots 2$$

Basically, we notice the dependence of the excitation coefficient (k) on the incident wavelength and the absorption coefficient (α), which is related to the quality of the material. Figure 7 shows the effect of changing the weight ratios of TiO_2 on the extinction coefficient (k) in terms of wavelength (λ). The increasing in k value with increase in TiO_2 ratios may be due to the roughness of the membrane surface, which enhanced scattering losses and thus reduced transmission power, at 10wt%TiO_2 a different behavior is observed as it decreases at increasing in wavelength ,related to amount of TiO_2 homogenous diffusion polymer chains .

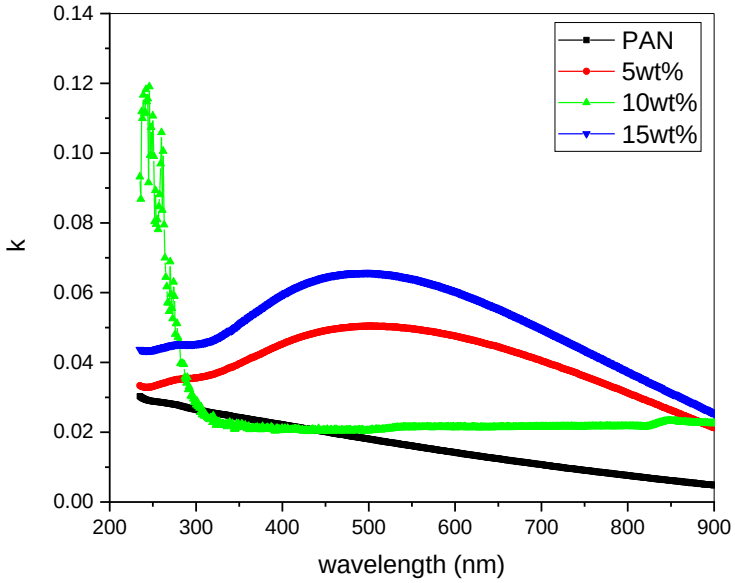

Figure 7: The relationship between excitation coefficient (k) and wavelength (λ) of PAN and PAN/TiO_2 nanofibers

The real part of refractive index (n) is calculated from the Fresnel reflectance equation at the air/film interface where the substrate effect is considered to be canceled out by the appropriate calibration [15].

$$n = \frac{1+R}{1-R} + \sqrt{\frac{2R}{(1-R)^2} + k^2} \qquad \ldots\ldots 3$$

This gives: The wavelength dependencies of (n) are shown in Fig. 8 at a wavelength range between (200-900) nm. Figure 8 shows a decrease in the refractive index (n) when increasing the wavelength of the studied films. The value of refractive index (n) at 327nm were about (1.32,1.19,1.34,1.33) of PAN and PAN/TiO_2 respectively , and these agreement with another study by W. Matysiak[16] were found the value of n about (1.34) of PAN and (1.55-1.73) of PAN/TiO_2 nanofibers using ellipsometery technique.

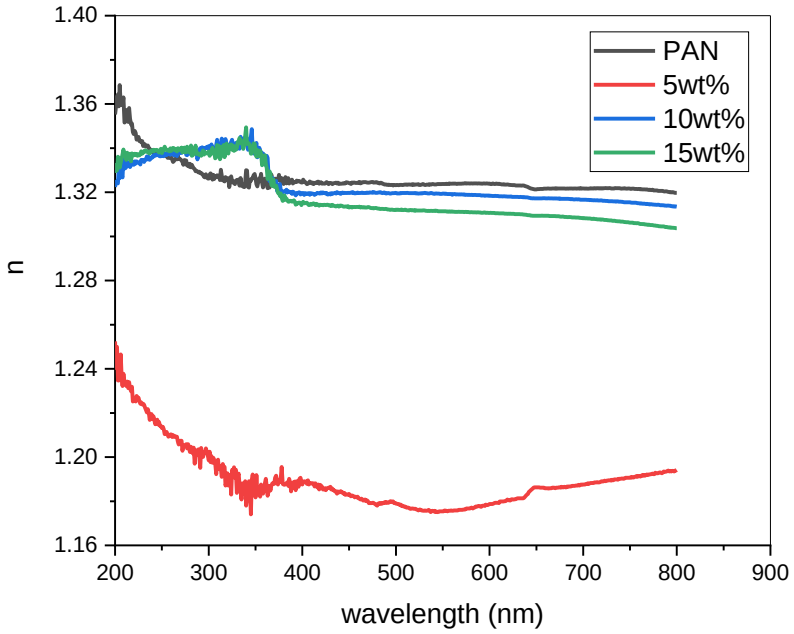

Figure 8: Refractive index (n) in significance of wavelength (λ) of PAN and PAN/TiO_2 nanofibers

To calculate the energy gap of composite nanofibers we use UV-Vis spectra. The UV spectrum provides information on the energy gap of the material. The Tauc equation shows the relationship between the energy gap of a material and the absorption coefficient (α) [13]:

$$\alpha h\nu = A(h\nu - E_g)^r \text{.....4}$$

where A represents the transition probability parameters, hυ represents the energy of the incident photon, and r represents the nature of the transition, for r equals (1/2), what is known as the permitted direct transmission occurs, and when (2) the permitted indirect transmission . The type of electronic transitions is determined based on the value of the absorption coefficient $\alpha > 10^4$of the nanofibers, as we note that they are direct transitions[12, 15]. The Figure 9 shows the energy gap diagram of the nanofibers PAN and (PAN/TiO_2) with different weight ratios (5,10 and 15) wt% TiO_2. We notice that with an increase in the percentage of TiO_2, the band gap decreases, as the energy gap of PAN nanofibers changes from 3.92 eV to (3.72, 3.39, 3.19) eV with different weight ratios (5,10 and 15) wt% TiO_2, respectively. The shift of the energy gap of PAN when adding TiO_2 has been reported in many studies[12-18], the addition of TiO_2 to PAN leads to a narrowing of the energy gap due to Fermi energy conversion near the conduction band[13].

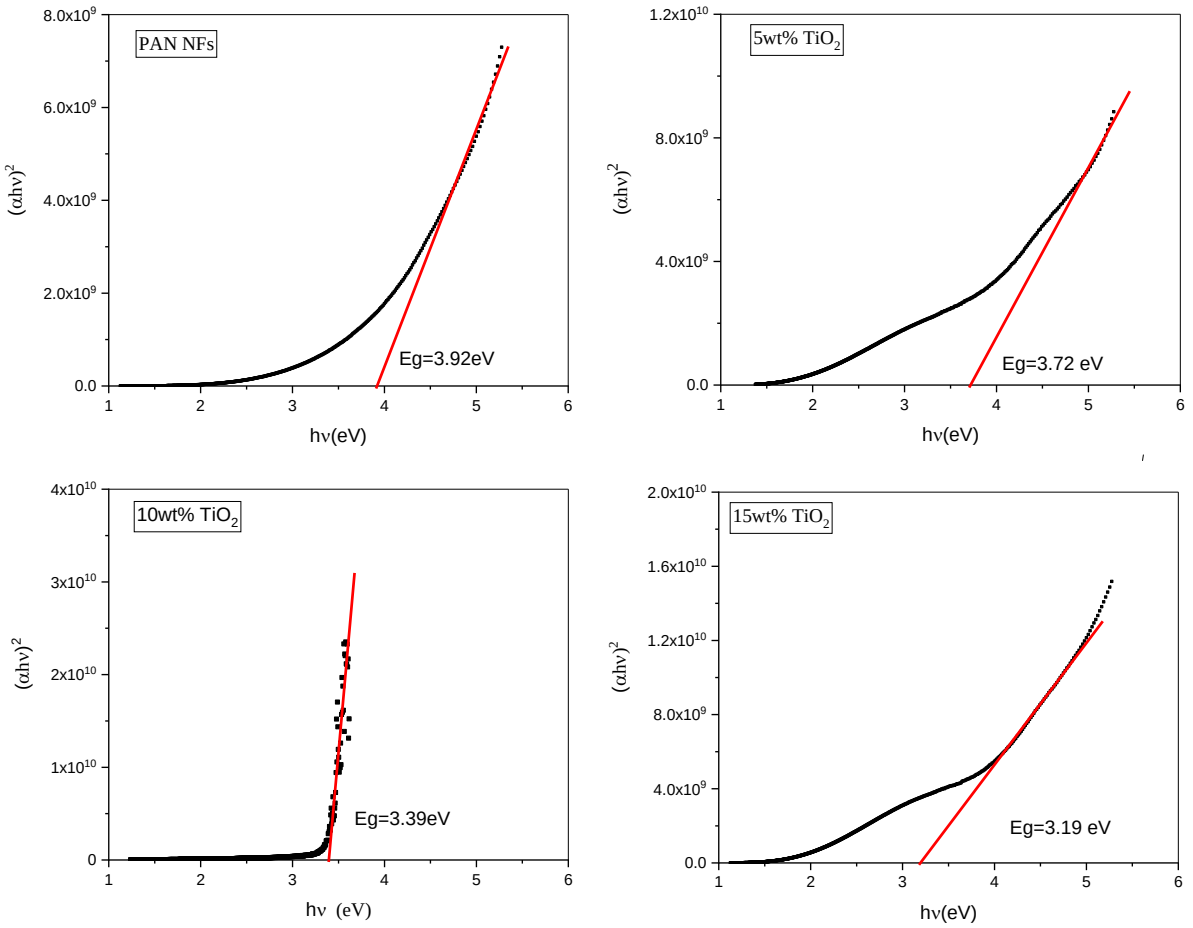

Figure 9: Band gap energy plots of PAN and PAN/TiO_2 nanofibers

The absorption coefficient (α) near the band edge appears to be exponentially dependent on the photon energy (hν). This is due to the use of the relation achieved from the residuals of the Urbach energy that characterizes the optical absorption in this material. From Urbach's experimental law, the Urbach energy (E_u) of the optical absorption edge in the material was calculated [16]:

$$\alpha(\upsilon) = \alpha_o e^{\frac{h\nu}{Eu}} \qquad \ldots\ldots 5$$

whereas E_u is the Urbach energy tail and α_o is a constant. The origin of E_t can be considered as thermal vibrations in the lattice[16]. The exponential dependence of (α) on (hυ) for the film indicates that it obeys Urbach's formula[17]. Figure 10 shows the logarithm α versus photon energy for the nanofiber membrane of PAN and PAN/TiO_2. The inverse of the slope at the linear part of the E_t curve represents, the magnitude of the Urbach tail (E_u) were (0.367,0.431,0.655 and

0.544)eV of PAN and PAN / TiO_2 nanofibers at different weight ratios respectively . we noticed large value of E_u at 10wt% TiO_2 because of TiO_2 were homogenous embedded between polymer chains .

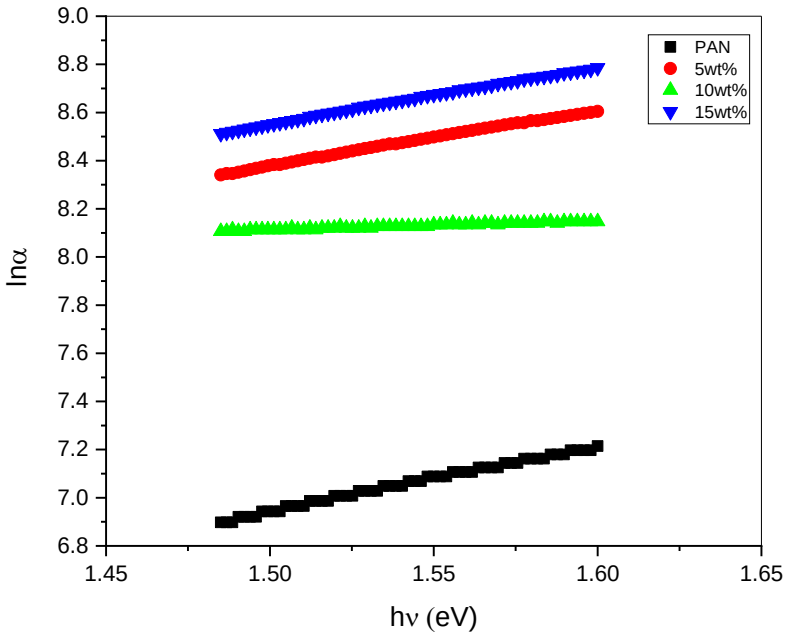

Figure 10: Urbach tail(E_u) as a function of photon energy(hν) of PAN and PAN /TiO_2 nanofibers.

For any solid material, the polarizability is proportional to the complex dielectric constant (ε*). Thus, ε* is an important quantity in the design of highly efficient optoelectronic devices[18]. According to the equations, the dielectric constant ε_r is determined[19]:

$$\varepsilon^* = \varepsilon_1 - i\varepsilon_2$$
$$\varepsilon_1 = n^2 - k^2 \qquad \text{.....6}$$
$$\varepsilon_2 = 2nk$$

Where, ε_1 is the real part and ε_2 is the imaginary part of the dielectric constant. The relationship between ε_1 and ε_2 and photon energy (hν) of PAN and PAN /TiO_2 nanofiber films are given in Figur 11 . We notice, As the photon energy increases, the magnitude of ε_1 and ε_2 increases ; The imaginary part (ε_2) is less than the real part (ε_1) of the dielectric constant. The dielectric constant ε_1 shows a value (1.75,1.40,1.79,1.79) at a photon energy 3.27eV , While imajanary part ε_2 is

small than real part is about (0.06,0.10,0.056,0.149) of PAN and PAN/TiO_2 nanofibers respectively .

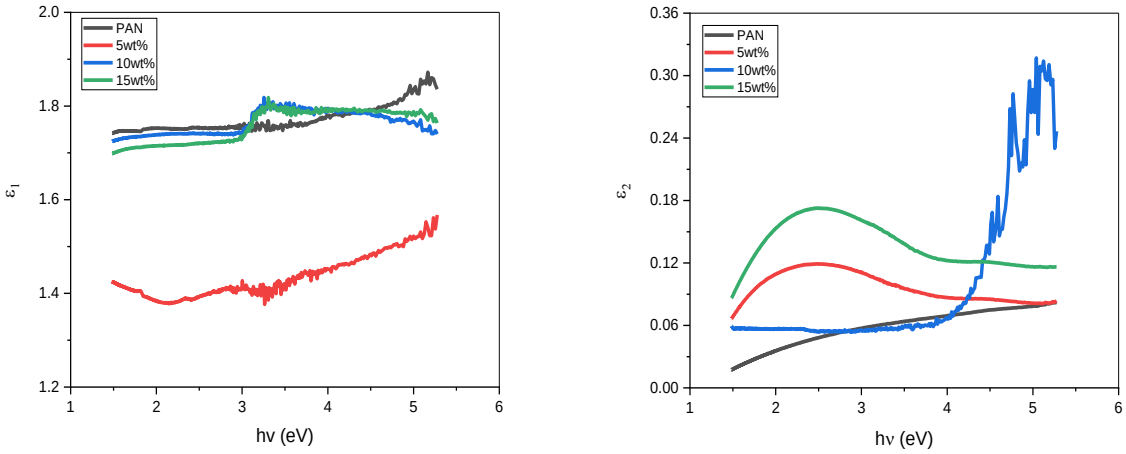

Figure 11: Real (ε_1) and imaginary (ε_2) parts of the complex dielectric function $\varepsilon(h\nu)$ of PAN and PAN/TiO_2 nanofibers at different ratios

Both the size and the surface energy loss are proportional to the characteristic decrease in energy of the fast electrons that transport the bulk of the material and its surface, respectively. From the real and imaginary parts of complex dielectric function we can calculated the volume energy loss function (VELF) and surface energy loss function (SELF). The SELF and VELF using the equations below we are able to determine the energy loss [21]

$$VELF = -Im\left[\frac{1}{\varepsilon}\right] = \frac{\varepsilon_2}{\varepsilon_1^2+\varepsilon_2^2} \quad \ldots\ldots\ldots\ldots\ldots \quad 7$$

$$SELF = -Im\left[\frac{1}{\varepsilon+1}\right] = \frac{\varepsilon_2}{(\varepsilon_1+1)^2+\varepsilon_2^2} \ldots\ldots \quad \ldots\ldots 8$$

Figure 12 shows the functions of volume and decrease in surface energy of PAN and PAN /TiO_2 thin films. SELF is lower than VELF .This implies that the energy of free charge carriers travelling at a surface, we also noticed that variation of SELF and VELF the same trend in increasing and decrease after that rapidly increase with increase TiO_2 weight ratios .The energy loss functions peak at 2.5eV of PAN and PAN/TiO_2 with ratios 5% and 15% ,but at 10% reveal to peak at 5eV corresponding to the interbond transitions[20].

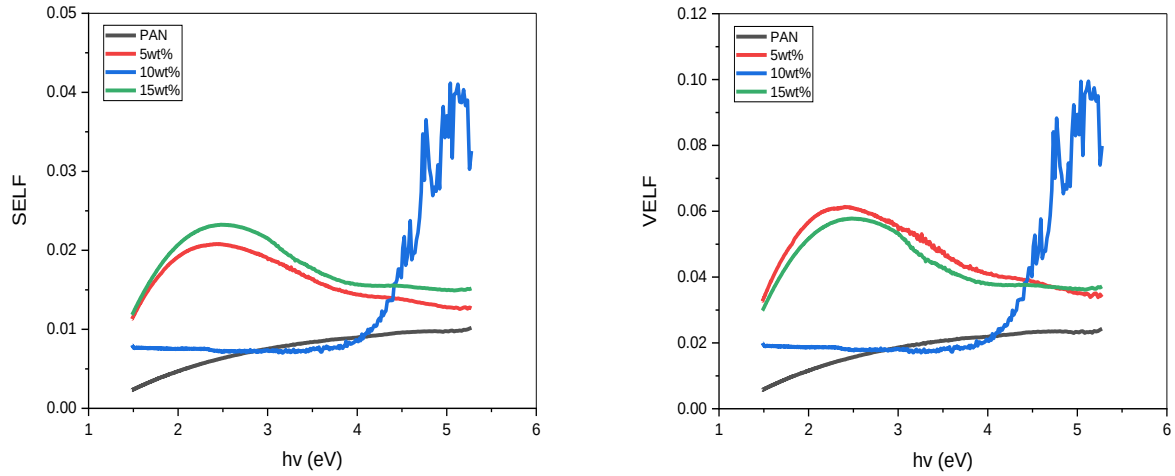

Figure 12: Surface and volume energy loss functions of PAN and PAN/TiO_2 nanofibers at different ratios

4. Conclusions

PAN nanofibers were produced via an electrospinning procedure. This approach was employed in the study to produce PAN nanofibers since it is affordable, easy to use, and environmentally benign. In order to employ PAN/TiO_2 composite nanofiber thin films in the field of optoelectronic devices, optical characteristics have been investigated. Furthermore, the dispersion of the PAN/TiO_2 nanocomposite fibers is amorphous. The PAN/TiO_2 composite nanofibers' absorption and reflection coefficients were computed in the spectral range of 200–900 nm. Using Tauc's curve, it was shown that the optical energy gap value of direct transmission of PAN nanofibers decreased as the TiO_2 weight ratio increased, from 3.92 eV to 3.19 eV at a 15% ratio of TiO2. SELF and VELF, two optical constants for PAN/TiO_2 nanofibers, were evaluated based on the results of the dielectric calculations. At 10wt% TiO_2, its maximum value is 5eV. Determine a PAN/TiO_2 composite fiber membrane's photovoltaic characteristics for usage in optoelectronic applications.

References

[1] K. Garg , G.L. Bowlin, Electrospinning jets and nanofibrous structures., Biomicrofluidics, 5(2011) 13403, doi: 10.1063/1.3567097.

[2] C. G. Reyes, J. P. F. Lagerwall, Disruption of electrospinning due to water condensation into the Taylor cone, ACS Appl. Mater. Interfaces, 12(2020) 26566–26576, https://doi.org/10.1021/acsami.0c03338

[3] S.S.S. Bakar, K.C. Fong, A. Eleyas, M. F. M. Nazeri, Effect of Voltage and Flow Rate Electrospinning Parameters on Polyacrylonitrile Electrospun Fibers, IOP Conf. Ser. Mater. Sci. Eng., 318(2018)1-7, doi: 10.1088/1757-899X/318/1/012076

[4] A. Haider, S. Haider, I. K. Kang, A comprehensive review summarizing the effect of electrospinning parameters and potential applications of nanofibers in biomedical and biotechnology, Arab. J. Chem., 11(2018)1165–1188, https://doi.org/10.1016/j.arabjc.2015.11.015

[5] A. Luraghi, F. Peri, L. Moroni, "Electrospinning for drug delivery applications: A review," J. Control. Release,. 334(2021) 463–484, doi: 10.1016/j.jconrel.2021.03.033.

[6] J. Xue, T. Wu, Y. Dai, Y. Xia, "Electrospinning and electrospun nanofibers: Methods, materials, and applications," Chemical Reviews, American Chemical Society, 119 (2019) 5298–5415, https://doi.org/10.1021/acs.chemrev.8b00593.

[7] B. Fryczkowska, Z. Piprek, M. Sieradzka, R. Fryczkowski, J. Janicki, Preparation and Properties of Composite PAN/PANI Membranes, Int. J. Polym. Sci., (2017)1-14, doi: 10.1155/2017/3257043.

[8] S. Shree, I. Paradisanos, X. Marie, C. Robert, B. Urbaszek, "Guide to optical spectroscopy of layered semiconductors, Nat. Rev. Phys., 3(2021) 39–54, doi.org/10.1038/s42254-020-00259-1

[9] W. Zhang, B. Zaarour, L. Zhu, C. Huang, B. Xu, X. Jin, A comparative study of electrospun polyvinylidene fluoride and poly(vinylidenefluoride-co-trifluoroethylene) fiber webs: Mechanical properties, crystallinity, and piezoelectric properties, J. Eng. Fibers Fabr., 15(2020)1-8, **https://doi.org/10.1177/1558925020939290**

[10] C. A. Bode-Aluko,O. Pereao,H.H. Kyaw,S. Dobretsov, Materials Science & Engineering B Photocatalytic and antifouling properties of electrospun TiO_2 polyacrylonitrile composite nanofibers under visible light, Mater. Sci. Eng. B, 264(2021)114913, https://doi.org/10.1016/j.mseb.2020.114913

[11] M. Mirjalili, S. Zohoori, Review for application of electrospinning and electrospun nanofibers technology in textile industry, J Nanostruct Chem,6(2016)207–213, doi: 10.1007/s40097-016-0189-y

[12]C. G. Reyes,J. P. F. Lagerwall,, Disruption of Electrospinning due to Water Condensation into the Taylor Cone, ACS Appl. Mater. Interfaces, 12 (2020) 26566–26576, doi: https://doi.org/10.1021/acsami.0c03338.

[13] S. Hartati , A. Zulfi , P.Y.D. Maulida ,A. Yudhowijoyo,M. Dioktyanto ,K. E. Saputro, A. Noviyanto , N.T. Rochman, Synthesis of Electrospun PAN/TiO_2/Ag Nanofibers Membrane As Potential Air Filtration Media with Photocatalytic Activity, ACS Omega, 7(2022) 10516–10525, doi.org/10.1021/acsomega.2c00015

[14] K. Alfaramawi, "Optical and dielectric dispersion parameters of general purpose furnace (GPF) carbon black reinforced butyl rubber," Polym. Bull., 75(2018) 5713–5730, doi.org/10.1007/s00289-018-2353-7

[15] S.K.J. Al-Ani , Y. Al-Ramadin , M.S. Ahmad, A.M. Zihlif , M. Volpe , M. Malineonico , E. Martuscelli , G. Ragosta, The optical properties of polymethylmethacrylate polymer dispersed liquid crystals, Polymer Testing 18 (1999) 611–619, doi.org/10.1016/S0142-9418(98)00059-2

[16] F. Urbach, "The long-wavelength edge of photographic sensitivity and of the electronic absorption of solids, Phys. Rev., 92(1953) 1324, doi.org/10.1103/PhysRev.92.1324.

[17] C. Zaouche, A. Gahtar , S. Benramache , Y. Derouiche , M. Kharroubi , A. Belbel , C. Maghni , L. Dahbi ," The determination of urbach energy and optical gap energy by many methods for Zn doped NiO thin films fabricant semiconductor by spray pyrolysis", Dig. J. Nanomater. Bios.,17(2022)1453-1461, doi.org/10.15251/DJNB.2022.174.1453

[18] A. A. M. Farag ,I. S. Yahia, Structural, absorption and optical dispersion characteristics of rhodamine B thin films prepared by drop casting technique, Opt. Commun., 283(2010) 4310–4317, doi.org/10.1016/j.optcom.2010.06.081

[19] M.M. El-Nahass, A. M. Farid, A. A. Atta, Structural and optical properties of Tris (8-

hydroxyquinoline) aluminum (III)(Alq3) thermal evaporated thin films, J. Alloys Compd., 507(2010) 112–119, https://doi.org/10.1016/j.jallcom.2010.07.110

[20] M. Cardona, M. Weinstein, G. A. Wolff, Ultraviolet reflection spectrum of cubic CdS, Phys. Rev., 140(1965)633, doi.org/10.1103/PhysRev.140.A633

[21] M.S. Ebied , M. Dongol, M. Ibrahim, M. Nassary, S. Elnobi, A. A. Abuelwafa," Structural and Optical Properties of Nanocrystalline 3-(2-Benzothia zolyl)-7-(diethylamino) Coumarin (C6) Thin Films for Optoelectronic Application, J . Electr.Mater.,51(2022)5770–5782 doi.org/10.1007/s11664-022-09792-4.

الخواص البصرية لألياف البولي أكريلونترايل / ثاني اوكسيد التيتانيوم النانوي المحضرة بطريقة الغزل الكهربائي

فرح محمد راضي [1] ، وداد صالح حنوش [2] ، علي قاسم عبد الله [3]

[1,3] قسم الفيزياء ، كلية العلوم ، جامعة البصرة ـ العراق

[2] قسم الكيمياء ـ كلية العلوم ـ جامعة البصرة ـ العراق

المستخلص

في هذا العمل ، تم تحضير البولي أكريلونترايل (PAN) وثاني أكسيد التيتانيوم (TiO_2) النانوي بنسب وزنية مختلفة تتراوح بين (5 ، 10 ، 15)% من TiO_2 بواسطة البلمرة في الموقع. تم استخدام تقنية الغزل الكهربائي لتحضير ألياف نانوية من PAN/TiO_2 من محلول متجانس. أظهرت النتائج التي تم الحصول عليها من حيود الأشعة السينية أن الحالة العشوائية هي المهيمنة على التركيب البلوري. تم التحقيق في مورفولوجيا الألياف النانوية عن طريق المسح المجهري الإلكتروني (SEM) ، لوحظ ان الألياف المحضرة ذات اتجاهية عالية وبأقطار تتراوح بين 33 نانومتر بالنسبة الى PAN وحوالي بحدود 51 نانومتر الى متراكبات PAN/TiO_2 بنسبة 10%. تم قياس الخواص الضوئية لأغشية الألياف النانوية بواسطة جهاز المطياف الضوئي ضمن الاطوال الموجية (200-900) نانومتر ، وتم حساب فجوة الطاقة للأغشية الألياف النانوية ، حيث لوحظ هناك تناقص بقيمة فجوة الطاقة (Eg) مع زيادة نسبة الوزن للجسيمات النانوية TiO_2المضاف حيث انخفضت فجوة الطاقة من 3.92 الكترون فولت إلى (3.72 ، 3.39 ، 3.19) الكترون فولت للنسب الوزنية (5 ، 10 , 15)% من TiO_2 على التوالي ، وكذلك تم حساب العديد من البارامترات مثل: معامل الإثارة (k) ، معامل الانكسار (n), يول يورباخ (E_t) Urbach tails ، ثابت العزل (ε_1) ، فقدان العزل الكهربائي (ε_2) وكل من دالة فقد الطاقة الحجمية (VELF) وفقدان الطاقة السطحية (SELF).